Observed characteristics of Mozambique Channel eddies

N. C. Swart,[1,2] J. R. E. Lutjeharms,[1] H. Ridderinkhof,[3] and W. P. M. de Ruijter[4]

Received 4 October 2009; revised 19 March 2010; accepted 6 April 2010; published 8 September 2010.

[1] The flow in the Mozambique Channel is dominated by large, southward propagating, anti-cyclonic eddies, as opposed to a steady western boundary current. These Mozambique Channel eddies feed their waters into the Agulhas Current system, where they are thought to have a significant influence on the formation of the Natal Pulse and Agulhas Ring shedding. Here we use in situ hydrographic and nutrient data, together with satellite altimetry and surface velocity profilers to provide a detailed characterization of the Mozambique Channel eddies. Two warm eddies in the Channel at 20°S and 24°S had diameters of over 200 km. They rotated anti-cyclonically with a tangential velocity of over 0.5 $m.s^{-1}$. Vertical sections show that the eddies reached to the bottom of the water column. Relative to the surrounding waters, the features were warm and saline. The total heat and salt anomalies for the southernmost eddy were computed relative to a reference station close by. At 24°S the total anomalies were 1.3×10^{20} J and 6.9×10^{12} kg, respectively, being on par with Agulhas rings. Mozambique Channel eddies thus have the potential to form a major contribution to the southward eddy heat flux in the Agulhas Current system. The feature also had positive nutrient and negative oxygen anomalies. The large magnitude of the water mass anomalies within the eddy suggests that interannual variability in Mozambique Channel eddy numbers would have a significant impact on downstream water mass characteristics.

Citation: Swart, N. C., J. R. E. Lutjeharms, H. Ridderinkhof, and W. P. M. de Ruijter (2010), Observed characteristics of Mozambique Channel eddies, *J. Geophys. Res.*, *115*, C09006, doi:10.1029/2009JC005875.

1. Introduction

[2] The Mozambique Channel reaches from Cape Amber at the northern tip of Madagascar to the southern tip at 26°S, a length of some 1600 km. At the narrows with the African continent the channel is about 430 km wide, while at 20°S it reaches a maximum width of about 1000 km. The continental shelves on the Mozambican and Madagascan sides of the channel are in general narrow, and bordered by steep continental slopes. Constrained within this bathymetry, the flow field in the Mozambique Channel has been a matter of some contention. The picture derived from averaging ships' drift [*Michaelis*, 1923; *Lutjeharms et al.*, 2000] as well as coarsely averaged hydrographic data suggests a steady southward, western boundary current type of flow, traditionally known as the Mozambique Current [e.g., *Sætre and Jorge da Silva*, 1984; *DiMarco et al.*, 2002]. However, more recent cruise and satellite observations and data from moored current meters in the narrows of the Channel suggest a totally different scenario.

[3] Acoustic Doppler Current Profiler (ADCP) measurements from the Agulhas Current Sources Experiment (ACSEX) I [see *Ridderinkhof et al.*, 2001; *de Ruijter et al.*, 2006], did not show a steady Mozambique Current, but rather revealed a train of large eddies. These eddies were around 300 km in diameter, and reached to the bottom (>2000 m) of the Channel. Drifters and LADCP measurements showed that the features swirled anti-cyclonically, and were surface intensified. Net southward eddy propagation resulted in a rectified southward current on the western side of the channel, and a rectified northward current in the center of the Channel. No cyclonic eddies were detected on the cruise, and furthermore it was proposed that the cyclonic anomalies present in satellite altimetry were artifacts of the MADT (Mean Absolute Dynamic Topography), and in fact simply represent the absence of anti-cyclonic features [*de Ruijter et al.*, 2002].

[4] An array of current meters deployed across the narrows of the channel during ACSEX I in March 2000 has provided an almost 2-year time series of the variability there [*Ridderinkhof and de Ruijter*, 2003]. During the entire current meter deployment no permanent western boundary current was present on the African coast. Rather, the current meter observations were also dominated by large anti-cyclonic eddies. Eddy formation in the vicinity of the narrows occurred intermittently (9 times in 668 days; 4 times in the first year, 5 times in the following 10 months). These eddies divided the time series of the current measurements into two regimes - one of high current flow associated with the passage of an

[1]Department of Oceanography, University of Cape Town, Cape Town, South Africa.
[2]Now at School of Earth and Ocean Sciences, University of Victoria, Victoria, British Columbia, Canada.
[3]Royal Netherlands Institute for Sea Research, Texel, Netherlands.
[4]Institute for Marine and Atmospheric Research, Utrecht University, Utrecht, Netherlands.

0148-0227/10/2009JC005875

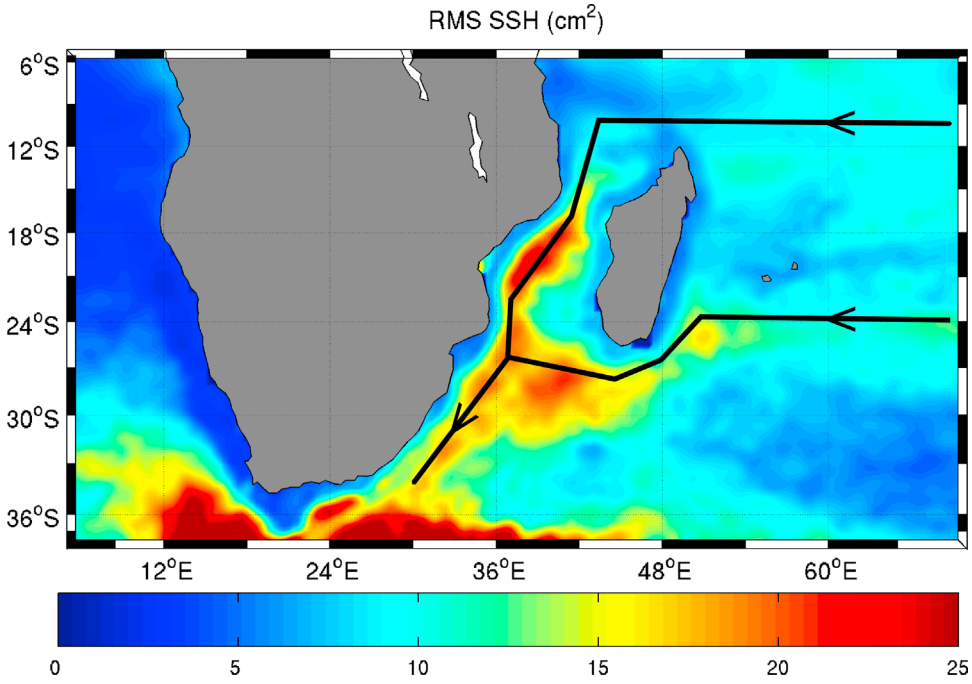

Figure 1. RMS of Mapped Sea Level Anomalies (cm^2) from altimetry of the broader South–West Indian Ocean region (6–35°S; 20–70°E), with annotations showing the propagation of perturbation from the Mozambique Channel downstream toward the Agulhas retroflection region. The two zonal arrows indicate the potential sources of these perturbations in the Mozambique Channel. To produce Figure 1, 11 years (1993/12/29–2004/12/29) of weekly gridded altimetry was used. No filtering to remove seasonality was applied.

anti-cyclone, and a low flow regime between eddies. During the passage of an eddy the flow through the channel exhibited large oscillations (between 20 Sv northward and 60 Sv southwards), but had a net southward component, with an average of 14 Sv. Such a volume flux would be approximately equivalent to 4 eddies per year with water trapping to 1500 m [*de Ruijter et al.*, 2002]. Recently, *Harlander et al.* [2009] have determined the volume transport through the moored array over the period November 2003–March 2005. They found a much smaller mean transport: 8.6 ± 14.1 Sv southward. Apparently, the transport through the Channel varies inter-annually. Also over this period the temporal variability in the currents was dominated by a period of 68 days. That period was related to the formation of southward migrating eddies. The triggering of the eddy formation is most presumably related to a westward migrating signal that may be a baroclinic Rossby wave channel mode with a period of about 70 days. The current meter observations were reported to contain no seasonality in the mean flow, or in the frequency of eddy shedding. Although the recent observations dispel the traditional concept of a steady, strong western boundary current flowing along the Mozambican side of the channel, the episodic and transient appearance of such a feature, as suggested by some numerical models [*Biastoch and Krauss*, 1999], cannot be ruled out entirely.

[5] Satellite altimetry provides more complete information on annual eddy numbers and eddy propagation than isolated cruise and sparse current meter data. Analyses of SSH (Sea Surface Height) data reveals that in the region north of the narrows eddies occur with a frequency of 7 per year (55 day period) [*Schouten et al.*, 2003]. Further south, near the center of the channel, the dominant frequency is 5 per year, and it reduces even more toward the southern end of the channel [*Schouten et al.*, 2002b, 2003]. This reduction in frequency may be associated to some degree with eddy dissipation near 20°S, and a merging of eddies to form larger features. However, the 5 and 7 per year modes both have local maxima near the northern entrance to the channel, indicating that they are not isolated from each other. Chlorophyll-a imagery also reveals a 5–6 per year frequency within the Channel proper [*Quartly and Srokosz*, 2004]. The eddies have been observed to propagate southward at about 3–4 km/day in the north (18–21°S), with higher speeds of 6 km/day in the south (22–27°S) [*Schouten et al.*, 2003].

[6] The 55 day period northwest of Madagascar is associated with waves of a length scale of around 400 km. These are probably related to a barotropic instability in the free jet extension of the South Equatorial Current (vide Figure 1) [*Schouten et al.*, 2003]. The high-resolution, numerical model experiment of *Biastoch and Krauss* [1999] found a similar formation mechanism, with a similar frequency, for the formation of the model eddies. The 4 per year signal characteristic of the southern Channel is the dominant frequency in a band around 24°S that stretches across the entire south Indian Ocean (vide Figure 1) [*Schouten et al.*, 2002b]. This variability is related to westward propagating baroclinic Rossby waves, which are probably triggered by baroclinic instability of the recently discovered Subtropical Indian Ocean Countercurrent (SICC) [*Siedler et al.*, 2006, 2009; *Palastanga et al.*, 2007]. Variability in this frequency band shows large elongated structures in the Mozambique Channel. These elongated features may be connected to the Rossby

waves coming in from the east around 24°S (Figure 1), and entering the channel via a Kelvin wave around the island of Madagascar that sheds Rossby waves from the western side of the island [*Schouten et al.*, 2003]. An alternative explanation may be the one associated with the baroclinic Rossby wave channel modes mentioned earlier [*Harlander et al.*, 2009]. Note that the latter explanation does not require any remote forcing.

[7] Mozambique Channel eddies potentially control Agulhas Ring shedding in two distinct ways (Figure 1) - the first is by triggering the formation of the Natal Pulse at the Natal Bight on the east coast of South Africa [*de Ruijter et al.*, 1999b; *van Leeuwen et al.*, 2000] and the second is by propagating down to the Agulhas Retroflection region, and initiating Ring shedding there [*Schouten et al.*, 2002a]. Furthermore, the Mozambique Channel has been identified as a non-negligible source of the Agulhas Current water [*Biastoch and Krauss*, 1999; *de Ruijter et al.*, 2002; *Donohue and Toole*, 2003; *Ridderinkhof and de Ruijter*, 2003], and a route for perhaps as much as 50% of the water entering the Indian Ocean through the Indonesian Throughflow. Moreover, it now seems clear that the net southward volume transport through the channel is modulated by the large anticyclonic eddies rather than a steady, narrow and intense Mozambique Current [*Biastoch and Krauss*, 1999; *de Ruijter et al.*, 2002; *Ridderinkhof and de Ruijter*, 2003].

[8] These eddies must then transport water mass properties into the Agulhas Current [e.g., *Roman and Lutjeharms*, 2009] that effect a heat and salt transfer, which is eventually fed into the Atlantic Ocean via Agulhas Rings [e.g., *Roman and Lutjeharms*, 2007], and ultimately contributing to the Meridional Overturning Circulation. Thus the heat and salt transport of the Mozambique Channel eddies is potentially globally significant [*Gordon*, 1985; *Weijer et al.*, 1999; *Biastoch et al.*, 2008a, 2008b]. However, coarse resolution numerical models (Figure 8) [*Jayne and Marotzke*, 2002] do not show a southward divergent eddy heat flux through the Mozambique Channel. Despite the suggestions of its significance, the Mozambique Channel eddies potential for heat and salt transport has not yet been observationally quantified, and the question of their contribution to the southward flux remains unresolved. In order to make an initial determination of whether the eddies are capable of influencing the heat and salt budgets of the Agulhas Current system we quantify the heat and salt anomalies in one eddy that we have observed. We also compute nutrient anomalies, and provide a general characterization of the eddies using the full ACSEX I CTD and bottle data, complemented by Surface Velocity Profilers (SVPs) and satellite altimetry.

2. Data and Methods

2.1. Cruise and Altimetric Data

[9] Continuous CTD and discrete Niskin bottle samples were collected in the Mozambique Channel between 26 March and 8 April 2000 as part of the first ACSEX cruise. Data were collected on four zonal sections, at 24°S, 20°S, 17°S and 12°S, each of which covered a portion of the Channel. Continuous CTD data were collected with a Seabird 911 CTD system to near the bottom (<5 m off the bottom) at each station. Bottle samples were collected at standard sampling depths using a 25 position rosette sampler. Water samples collected from the rosette were analyzed on a Guildline Autosal 8400A salinometer, and values used to calibrate the CTD. Oxygen concentrations of discrete samples were determined by a spectrophotometer Winkler technique. The discrete nutrient concentrations were determined colorimetrically on a Technicon TRAACS 800 autoanalyzer, following the methods of *Grasshoff et al.* [1983]. Full details are available in the cruise report by *Ridderinkhof* [2000]. The nutrient and oxygen data were interpolated from the standard depths to a 1 m vertical grid using a linear interpolation.

[10] LADCP data were also collected and have been reported by *de Ruijter et al.* [2002]. Eight standard WOCE/TOGA mixed layer type ARGOS drifters, with a holey sock drouged at 15 m, were also deployed during the cruise. Several of these were deployed within anti-cyclonic eddies. The quality controlled, 6 hourly interpolated data for these drifters were downloaded from the NOAA Drifter Data Assembly Center (http://www.aoml.noaa.gov/phod/dac/dacdata.html).

[11] Maps of Sea Level Anomalies (MSLA) and maps of absolute geostrophic velocities (MAGV) have been used here to further investigate the Mozambique Channel eddies observed in situ during ACSEX I. We have used the reference versions of the gridded, delayed time, merged products produced by Ssalto/Duacs and distributed by AVISO with support from CNES (http://atoll-motu.aviso.oceanobs.com/). The absolute geostrophic velocities are based on the Rio05 mean dynamic topography, referenced to the geoid.

2.2. Heat, Salt, and Nutrient Anomaly Calculations

[12] The Available Heat Anomaly (AHA) and Available Salt Anomaly (ASA) of the eddies have been calculated using the method developed by *Joyce et al.* [1981], and subsequently used by several authors [e.g., *Peterson et al.*, 1982; *Morrow et al.*, 2004; *Swart et al.*, 2008]. Density is used as a vertical coordinate since it "is helpful in separating horizontal variations of water masses from changes in the vertical position of density surfaces associated with eddy available potential energy (APE)" [*Joyce et al.*, 1981, p. 1279]. A reference field is defined, and the temperature and salinity changes along isopycnals are examined. It is necessary to choose both a representative reference station and a sensible density range over which the comparisons are made. These choices are made in section 3.3. The anomalies are calculated for layers, defined by 0.1 σ_t increments. The available heat anomaly per unit area in each density layer is

$$\mathrm{AHA} = \rho C_p h(\mathrm{T} - \mathrm{Tr})\ \mathrm{J.m^{-2}}. \quad (1)$$

Here ρ is the density of seawater (1030 $\mathrm{kg.m^{-3}}$); C_p is heat capacity at constant pressure (4000 $\mathrm{J.kg^{-1}.K^{-1}}$); h is the thickness of the density layer (in m within the eddy); Tr is the average in situ temperature for the density layer at the reference station, °C; T is the average in situ temperature for the density layer at the eddy station, °C. Similarly the available salt anomaly per unit area in each density layer is

$$\mathrm{ASA} = 0.001\rho h(\mathrm{S} - \mathrm{Sr})\ \mathrm{kg.m^{-2}}. \quad (2)$$

Here Sr is the average salinity for the density layer at the reference station and S is the average salinity for the density

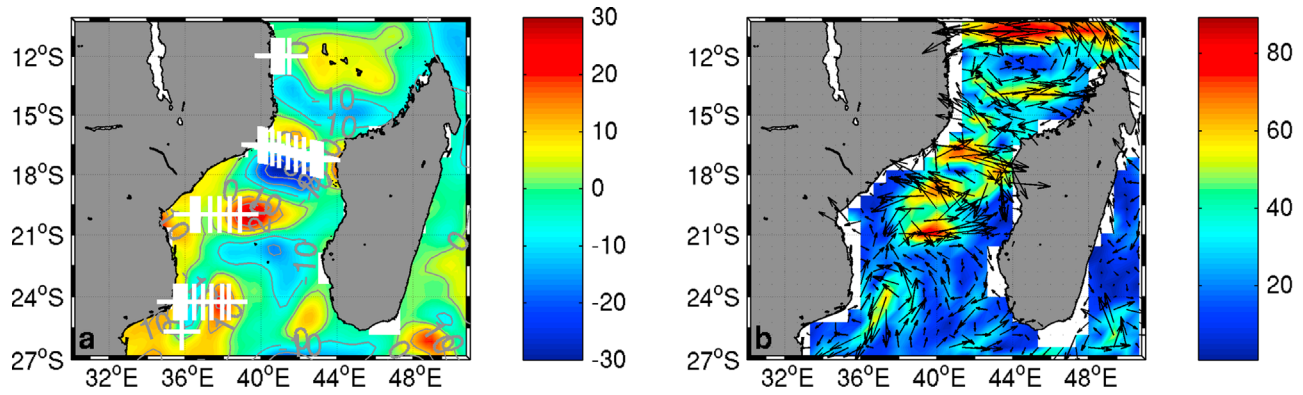

Figure 2. (a) Time-mean MSLA during ACSEX I cruise (units cm) and (b) contemporaneous absolute geostrophic velocities (units cm/s) from altimetry. The averaging period is 22 March – 12 April 2000. Lines of hydrographic stations undertaken during the cruise are marked by white plus symbols in Figure 2a.

layer at the eddy station. Additionally, nutrient anomalies were defined as

$$\mathrm{ANA} = \rho h(\mathrm{C} - \mathrm{Cr})\ \mu\mathrm{M.m}^{-2}. \quad (3)$$

Here C is the concentration of the nutrient within the eddy, μM.kg^{-1} and Cr is the concentration of the nutrient at the reference station, μM.kg^{-1}. The three sets of anomalies at each density layer could then be integrated radially with distance from the eddy center. The vertical sum of the integrated anomalies over all the density layers is then equal to the total heat, salt and nutrient anomalies associated with the eddy.

3. Results

3.1. Altimetry and Surface Drifter Data

[13] The time-mean MSLA field for the period surrounding the ACSEX I cruise (22/03/2000–12/04/2000) in the Mozambique Channel shows that positive sea level anomalies of over 20 cm were present at the positions of the hydrographic sections at 24°S and 20°S (marked in white in the MSLA plot in Figure 2; see auxiliary material for an expanded map of station positions).[1] Neither of the two sections completely traversed the two SLA features, but rather reached approximately to their centers. The altimetrically derived absolute geostrophic velocity field, also shown in Figure 2, reveals that the features were associated with strong anti-cyclonic circulations in their upper levels. The Mapped Absolute Geostrophic Velocities show that the Channel was dominated at the time by such mesoscale circulation features. The hydrographic data presented below and the LADCP data shown by *de Ruijter et al.* [2002] confirm that the positive SLA features were warm anti-cyclonic eddies. It is possible to estimate radii for these eddies based on the MSLAs, and for this purpose we subjectively choose the +10 cm MSLA to represent the edge of the eddies. Using this criterion the mean (of a meridional and zonal section through the eddy center) radii are approximately 100 km and 125 km for the eddies at 24°S and 20°S, respectively, somewhat smaller than the radii defined using LADCP data [*de Ruijter et al.*, 2002] and hydrography (below). To avoid aliasing caused by eddy propagation the gridded MSLA for the 29 March 2000 (not shown) was used in this calculation, as opposed to the mean altimetry for the whole cruise period.

[14] Figure 3 in turn shows the surface velocities recorded by two drifters released into the anti-cyclonic eddy at 24°S (see auxiliary material for the release positions and tracks). Also shown are the absolute geostrophic velocities derived from altimetry for the 7 day period centered on 29 March, the gridded data closest to the release of the drifters. The drifter that was closer to the edge of the eddy took around 7 days to complete a loop, with a diameter of about 170 km, at an average speed of 0.78 m.s^{-1}. The maximum velocity reached by this drifter during its first loop was 1.0 m.s^{-1} while it was in the northwest quadrant of the eddy, and it was slowest in the southeast. The second drifter, closer to the center, completed a loop with a diameter of about 75 km, reaching a maximum velocity of 0.95 m.s^{-1} in the northwest quadrant, and being slowest on average in the northeast. Traveling at a mean speed of 0.6 m.s^{-1} it completed the round trip in about 5 days.

[15] The altimetric absolute geostrophic velocities describe a similar picture of the anti-cyclonic flow, with velocities being greatest around the western edge of the eddy and reduced within its center. However, both the mean and maximum geostrophic velocities derived from the altimetry were lower than those given by even the slowest drifter, by 0.25 and 0.1 m.s^{-1}, respectively. The underestimation of surface current speed by about 0.2 m.s^{-1} by the altimetry is likely due to the fact the data used here are gridded and binned into a 7-day mean. Furthermore, ageostrophic processes that are not derivable from the satellite measurements may have influenced the drifters. Nonetheless, both the MAGV from altimetry and the surface velocities obtained from the drifters provide a clear view of the strong anti-cyclonic rotation of the feature.

3.2. Hydrographic Data

[16] The θ-S diagram shown in Figure 4 provides an overview of the water mass characteristics and their meridional variation in the Mozambique Channel at the time of the cruise (θ stands for potential temperature, referenced to the surface). Surface waters displayed a spread of characteristics,

[1] Auxiliary materials are available in the HTML. doi:10.1029/2009JC005875.

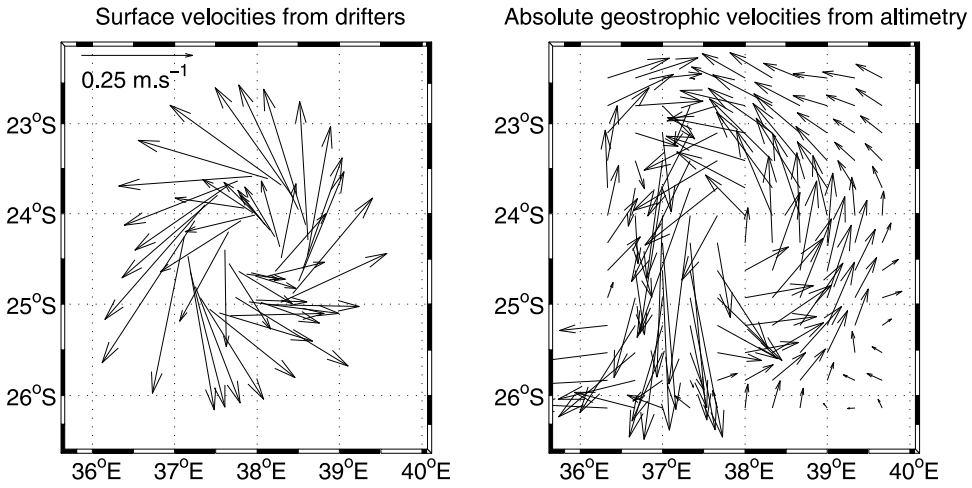

Figure 3. (left) Velocities from two surface drifters deployed during ACSEX I in an anti-cyclonic Mozambique eddy near 24°S, and (right) absolute geostrophic velocities associated with the eddy from altimetry. The drifter velocities were taken from the first loop of each drifter, which spanned the times 00:00 29/03–18:00 02/04, and 12:00 28/03–18:00 04/04, respectively. The MAGV are the 7-day gridded data centered on 29/03/2000.

typical of Tropical and Subtropical Surface Waters [*DiMarco et al.*, 2002; *Lutjeharms*, 2006]. The central waters were near uniform at all four sections, and showed a characteristic linear relation. By contrast at intermediate levels (around 5°C) waters showed a distinct meridional variation, with the Antarctic Intermediate Water (AAIW) in the south (red profiles) being considerably fresher than the Red Sea Intermediate Water (RSIW) to the north (black and green profiles) [*Clowes and Deacon*, 1935]. However, a freshening toward the south was not the case at every station. Several (red) profiles at 24°S were more saline, with values typical of the waters at 20°S. These few unusually saline stations in the south suggest a mixing of Antarctic Intermediate and Red Sea Intermediate Water masses and reflect the influence of the anti-cyclonic eddy in transporting RSIW southwards in an intermittent fashion. This agrees with recent findings by *Roman and Lutjeharms* [2007, 2009]. Those profiles extending into the Deep and Bottom waters tend to merge near a salinity of 34.8, and show little meridional or along-section variation. The deep (2500 m) oxygen maximum and local silicate minimum evident in the sections presented below suggests the presence of North Atlantic Deep Water there [*DiMarco et al.*, 2002; *van Aken et al.*, 2004]. The deepest profiles in the south also reached into slightly fresher, silicate-enriched Circumpolar Deep Water.

[17] The temperature, salinity, potential density and geostrophic velocity sections at 24°S, show the nature of the western half of the warm anti-cyclonic eddy located there at the time of the cruise (Figure 5a). Presented in Figure 5d are the geostrophic velocities computed from the temperature, salinity and pressure data, using the CSIRO seawater routine, and relative to the bottom. These computed geostrophic velocities reveal the vertical pattern of anti-cyclonic circulation associated with the eddy. Southward geostrophic velocities in the high-speed jet on the western edge of the eddy reached over 0.6 m.s^{-1}, similar to the LADCP measurements of *de Ruijter et al.* [2002], as well as the mean drifter velocities documented above. Thus the velocities from all these three methods are in qualitative agreement about the anti-cyclonic circulation within the eddy, although quantitative differences exist.

[18] Progressing east along the section, the isotherms, isohalines and isopycnals deepened significantly once the boundary of the eddy was crossed at around 36.5°E. The displacement of the isopleths is most significant in the upper part of the water column, being over 100 m, but the influence of the eddy, mentioned above, can be seen to extend right to the bottom. The barotropic nature of these anti-cyclonic Mozambique Channel eddies was also clearly borne out in the LADCP data [*de Ruijter et al.*, 2002]. Assuming that the section reached the center of the eddy, its radius appears to

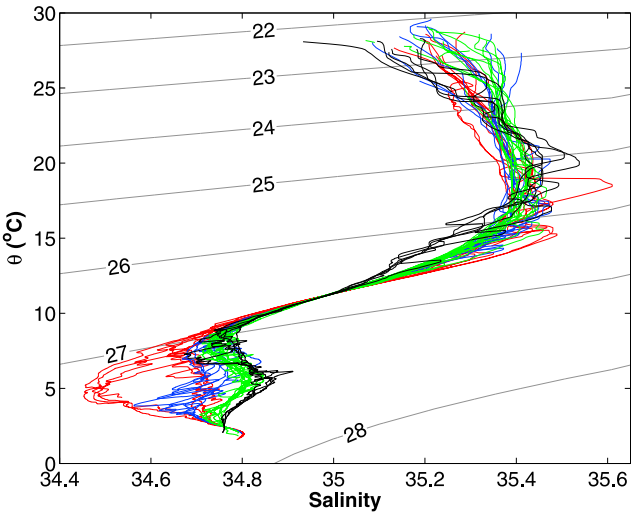

Figure 4. A θ-S diagram showing the water mass characteristics at 24°S (red), 20°S (blue), 17°S (green), and 12°S (black) during ACSEX I.

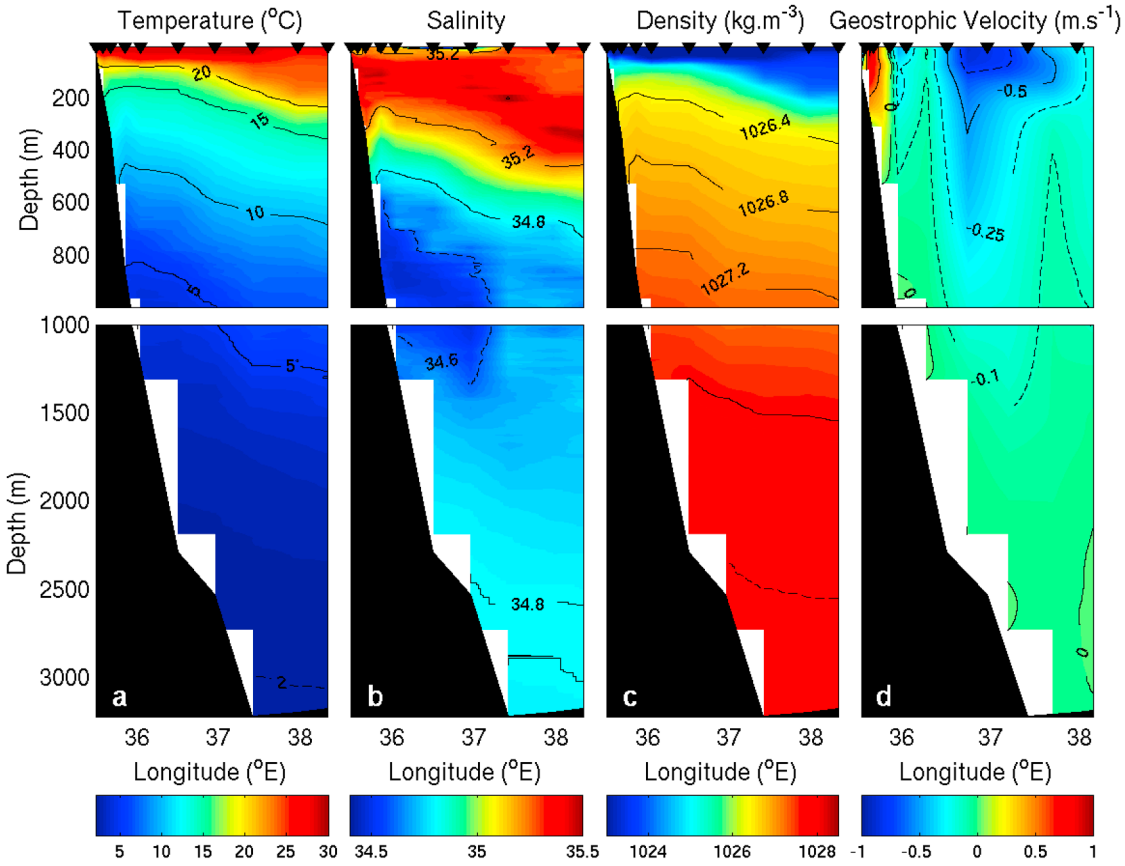

Figure 5. (a) Temperature, (b) salinity, (c) potential density, and (d) geostrophic velocity sections at 24°S, across one half of a Mozambique eddy. (top) The upper 1000 m, and (bottom) the 1000–3000 m depth range. See Figure 2 for a station map. Black triangles at the top mark the station positions.

have been about 110 km (36.5–38.3°E). This is in good agreement with the 100 km radius calculated from the altimetry above.

[19] Figure 6 displays the nitrate (Figure 6a), phosphate (Figure 6b), silicate (Figure 6c), and oxygen (Figure 6d) concentrations on the 24°S section. The nutrients were depleted to near zero in the surface waters, and increased in concentration with depth, a distinct nutricline being evident between 500 and 1000 m. There was a marginal deepening of the nutricline to the east, corresponding to the deepening of the thermocline caused by the presence of the warm anti-cyclonic eddy, however the deepening in the nutricline was not as pronounced. The vertical distribution of oxygen was more complex. An oxygen minimum of <140 μM, typical of Red Sea Intermediate Water, extended between 1000 and 1500 m, being most intense in the east of the section, in the center of the eddy. In the west of the section oxygen-rich AAIW was present. AAIW is know to be carried northward by the Mozambique Undercurrent at a depth of about 1000 m [*de Ruijter et al.*, 2002]. Oxygen maxima occurred very near to the surface, and at around 500 m, as well as below the oxygen minimum.

[20] The hydrographic characteristics of the 20°S section (vide Figure 2) are shown in Figure 7. A deepening of the temperature, salinity and density isopleths moving east along the section was also evident here. However, the deepening only occurred at the last two stations, east of 38°E. Comparison with the MSLA field in Figure 2 confirms that only the easternmost 2 stations at 20°S fell within the positive MSLA feature. The vertical displacement of the isopleths was therefore not as great as for the eddy at 24°S, but this is likely because the center of the feature at 20°S was not reached by the section. Nonetheless the calculated geostrophic velocities show the southward jet current on the eddy's western edge extending throughout the water column. Since the section did not reach to the center of the eddy, it is difficult to estimate the size of the eddy based only on the hydrographic data presented here. Thus we adopt an altimetrically derived radius of 120 km for the eddy at 20°S.

[21] The nutrient concentrations at 20°S displayed similar patterns to the section further south, with the nutricline again positioned between 500 and 1000 m (Figure 8). The nutrient concentrations all show a deepening of the nutricline at the easternmost two stations, corresponding to the location of the warm, anti-cyclonic eddy, although again the vertical displacement is less pronounced than that of the thermocline. The oxygen section reveals a similar vertical structure to that at 24°S, however the oxygen minimum near 1000 m is more intense, reaching below 100 μM, and is not displaced to the east. This may indicate a weakening of the Mozambique Undercurrent leading to reduced AAIW penetration to this latitude on this occasion. Numerical model simulations

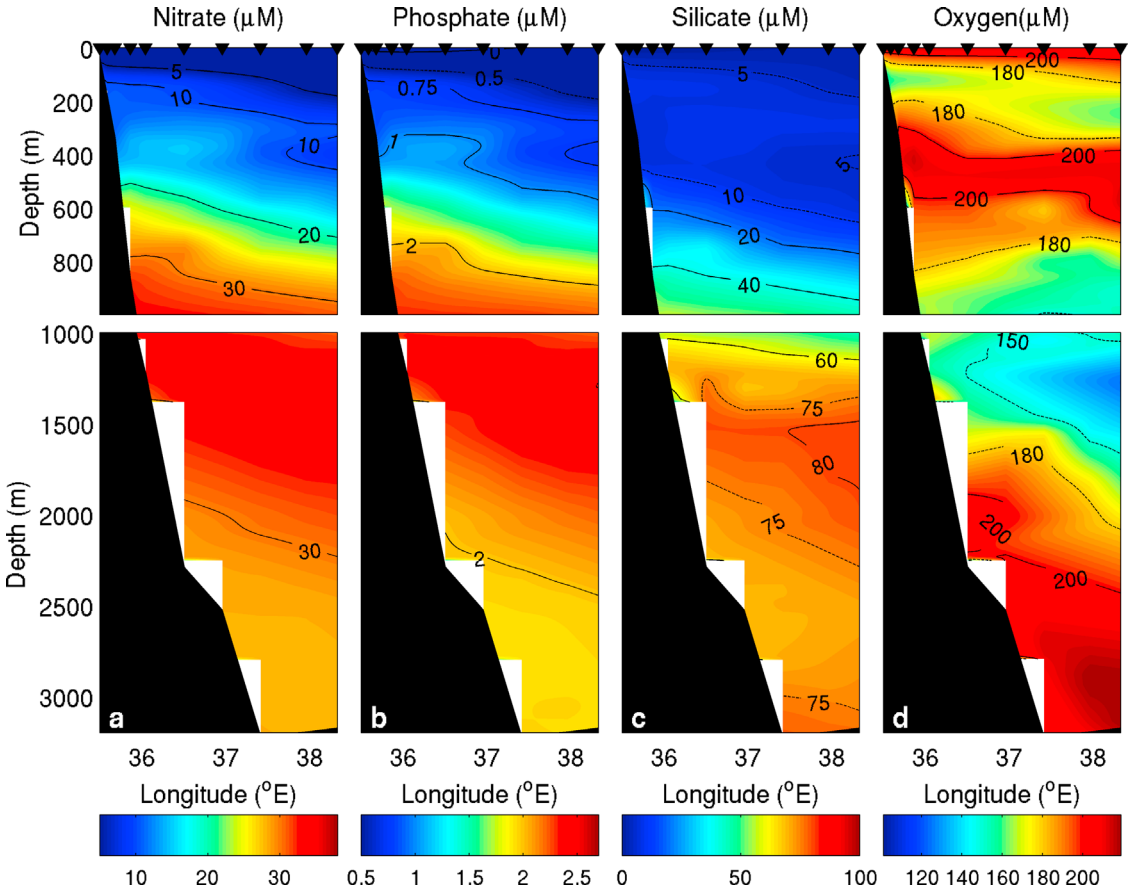

Figure 6. Vertical sections at 24°S, across half of a Mozambique eddy. Nitrate (a), phosphate (b), silicate (c) and oxygen (d), are all in μM. These may be compared to the physical parameters in Figure 5. (top) The upper 1000 m, and (bottom) the 1000–3000 m depth range. Black triangles at the top mark the station positions.

[*Biastoch et al.*, 2009] do not show such a meridional reduction over the long-term.

3.3. Temperature, Salinity, and Nutrient Anomalies

[22] Figure 9 shows θ-S diagrams for depths >400 m, of the sections at 24° (a) and 20°S (b). On the basis of the 10 cm MSLA (Figure 2), and their characteristics, the profiles were separated into eddy stations (red) and reference stations (blue). At 24°S, the easternmost three stations were deemed within the eddy, and on any one isopycnal were typically warmer and more saline than the surrounding water. Only the two easternmost stations fell within the eddy at 20°S. Along the isopycnals $27.0 < \sigma_t < 27.4$, these eddy stations were generally warmer and more saline than their surrounds. However, there were two warm and even more saline stations outside of the eddy to the west. These can be identified in Figure 7b as the salty core of water (S > 34.8) near 1000 m at 37.4°E.

[23] The temperature and salinity anomalies in the eddy at 24°S were computed as per section 2.2, where the blue profiles in Figure 9a were averaged to produce the reference station. The vertical cross section of the temperature anomalies is shown in Figure 10a. They were close to zero west of 37°E. The presence of the continental shelf is responsible for the absence of information at deeper isopycnals on the western edge of the section. The most prominent feature was associated with the anti-cyclonic eddy, which was represented by a strong temperature anomaly of over 6×10^8 J.m^{-2}. It is evident that the section only resolved the western portion of the anomaly associated with the eddy. The salinity anomaly showed a similar pattern, reaching over 20 kg.m^{-2} at its center. The greater part of the anomalies was confined between σ_t 27.0 and 27.6, in accordance with the separation of the profiles in Figure 9a. Figures 10c and 10d were produced by vertically summing the anomalies over all σ_t levels. These vertically summed anomalies are plotted against distance from the eastern edge of the section, which was assumed to be the center of the eddy.

[24] The vertically summed heat anomaly (Figure 10c) and salt anomaly (Figure 10d) were both a maximum at the eddy center, and then decreased slowly to around 100 km from the center, after which both anomalies underwent a rapid decay to near zero by 140 km from the center of the eddy. Such a rapid decay would be expected as the boundary of the ring was crossed. These summed anomalies were integrated horizontally, between the eddy center and where they decayed to zero around 140 km away. The resulting total available heat and

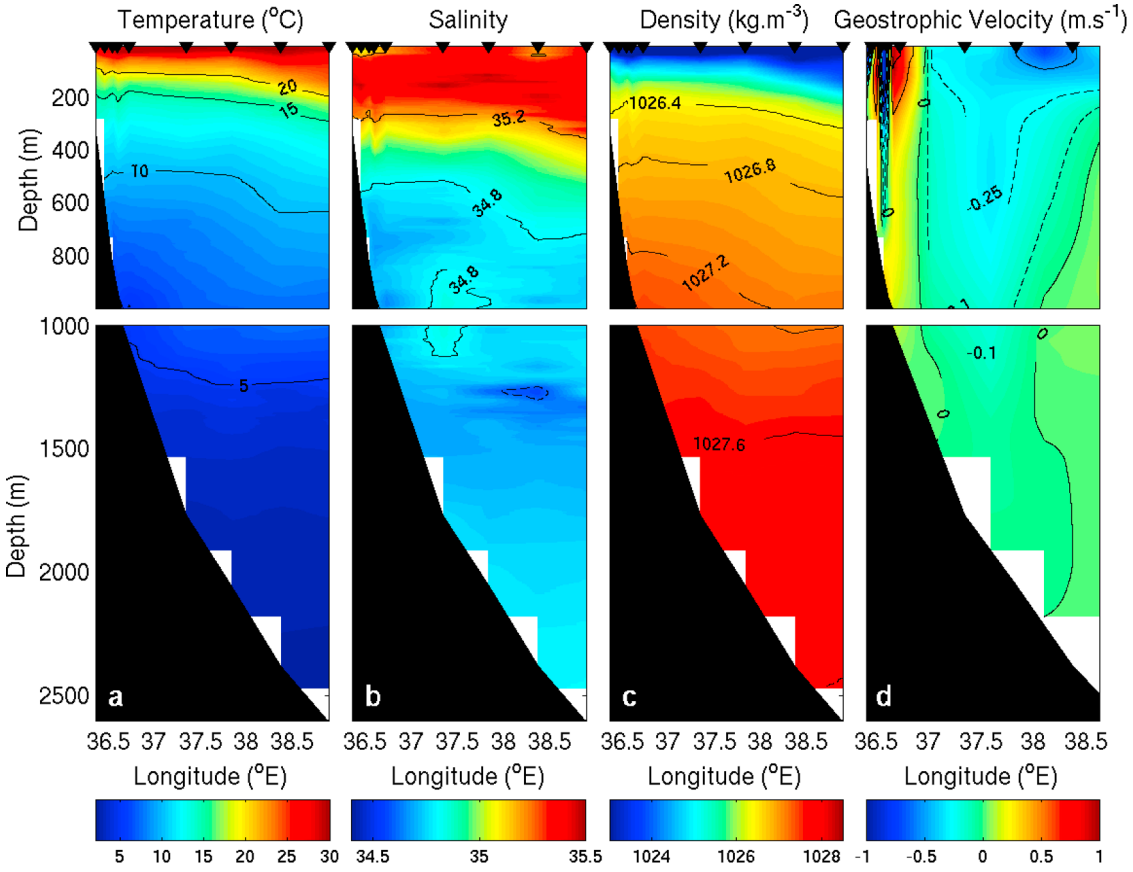

Figure 7. Temperature (a), salinity (b), potential density (c) and geostrophic velocity (d) sections across portion of an anti-cyclonic eddy in the Mozambique Channel at 20°S. See Figure 2 for a station map. (top) The upper 1000 m, and (bottom) the 1000–3000 m depth range. Black triangles at the top mark the station positions.

salt anomalies associated with the eddy were 1.3×10^{20} J and 6.9×10^{12} kg, respectively. The magnitude of these anomalies is large, being on a par with Agulhas Rings [*van Ballegooyen et al.*, 1994] and significantly in excess of those observed in other current systems such as the Antarctic Circumpolar Current [e.g., *Swart et al.*, 2008].

[25] The heat and salt anomaly were also computed for the 20°S section, using a reference station produced by averaging the blue profiles in Figure 9b. The result is shown in Figure 11. Positive heat and salt anomalies again occurred in the $27.0 < \sigma_t < 27.5$ range. However, here the anomalies were not clearly associated with the anti-cyclonic eddy on the eastern edge of the section, but were concentrated near the core of warm, saline waters around 1000 m at 37.4°E. These heat and salt anomalies were considerably lower than those at the section to the south already discussed (Figure 10). Since we were unable to identify the anomalies as clearly belonging to the anti-cyclone, we do not compute total heat and salt anomalies for the 20°S eddy.

[26] Using the same criterion for eddy versus reference stations as above, along-isopycnal nutrient and oxygen anomalies were calculated for the 24°S section (Figure 12). The dominant signal occurred below $\sigma_t = 27.0$, in accord with the hydrographic data. Here the eddy was enriched in nutrients, yet depleted in oxygen relative to the surrounding waters. At slightly shallower levels, around $\sigma_t = 26.5$, the eddy was in contrast in nutrient deficit and oxygen surplus relative to the reference station. This switch within the eddy from being low in nutrients (above 500 m), to being nutrient rich (below 1000 m), can also be observed by examining the eastern side of the section in Figure 6.

[27] As for the hydrography, the nutrient and oxygen anomalies were vertically summed and horizontally integrated to produce total nutrient and oxygen anomalies for the eddy. These are given in Table 1. The results indicate that overall, along isopycnal surfaces, the eddy was enriched in nutrients and depleted in oxygen relative to the surrounding waters. The resulting total nutrient anomalies do not conform to Redfield ratios. This reflects the fact that small deviations from Redfield stoichiometry in depth coordinates are amplified by the multiplication by layer thickness, h, in the isopyncal calculation (3). Nonetheless these total anomalies maybe sensitive to reference station choice, and the coarse sampling, and should be interpreted with caution.

[28] At any one depth in the upper 1000 m, the eddies were poor in nutrients relative to their surrounds. To highlight the difference between anomalies computed on isopycnals surfaces, and anomalies computed using depth coordinates, we show the average nutrient anomaly with depth in Figure 13.

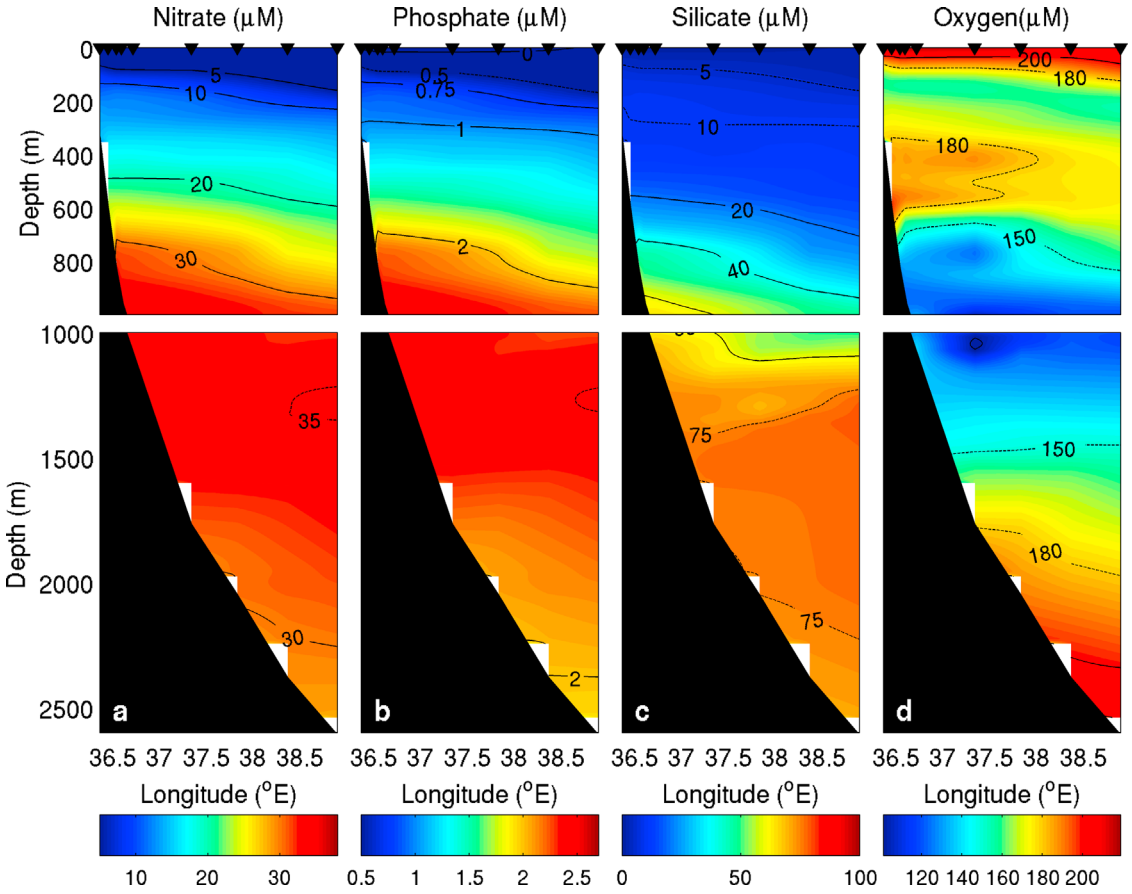

Figure 8. Vertical sections at 20°S, across part of a Mozambique eddy. (a) Nitrate, (b) phosphate, (c) silicate, and (d) oxygen, all in μM. These may be compared to the physical parameters in Figure 7. (top) The upper 1000 m, and (bottom) the 1000–3000 m depth range. Black triangles at the top mark the station positions.

These confirm the eddy to be depleted in nutrients on constant depth surfaces, in the upper 1000 m.

4. Discussion

[29] The hydrographic, altimetric and drifter data presented here, together with the LADCP data previously provided by *de Ruijter et al.* [2002], provide a coherent view of the eddies observed in the Mozambique Channel during ACSEX I. The features were 100–150 km in radius and exhibited strong anti-cyclonic rotation. At intermediate depths, the eddies typically contained RSIW, while the surrounding waters were cooler and fresher. The southward advection of warm, saline RSIW by the eddies is thus responsible for the separation between

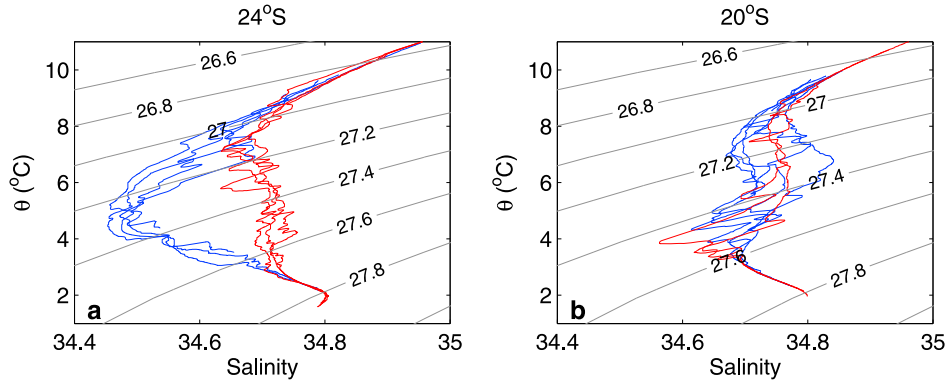

Figure 9. The θ-S diagrams, for depths >400 m, for the (a) 24°S and (b) 20°S sections. The stations inside the anti-cyclonic eddies on the eastern edges of the sections are shown in red. The remaining stations to the west (in blue) were averaged into reference stations to compute temperature and salinity anomalies (vide Figures 10 and 11). At 20°S two particularly warm, saline stations outside of the eddy tend to obscure its properties.

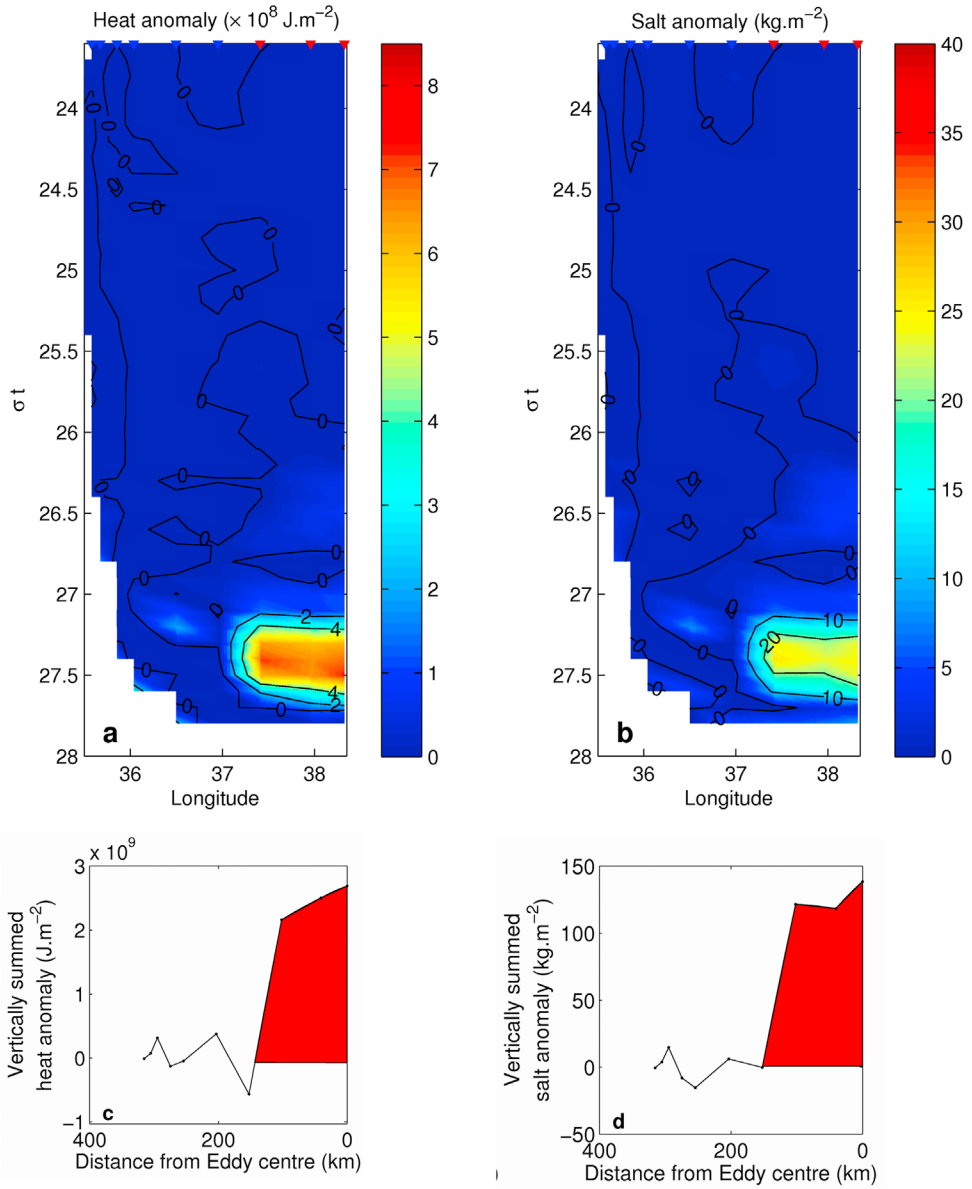

Figure 10. Vertical sections of (a) heat and (b) salt anomalies at 24°S, calculated using isopycnal coordinates. The vertically summed (c) heat and (d) salt anomalies with distance from the eastern edge of the section. The reference station against which the anomalies were computed was an average of the 7 westernmost stations on the section (blue triangles). The positions of the stations within the eddy are shown by red triangles. The anti-cyclonic eddy (vide Figures 2, 5, and 6) is evident in the positive heat and salt anomalies on the eastern side of the section.

the profiles at intermediate depths ($27.0 < \sigma_t < 27.6$) evident in Figure 9. This separation was only marginal at 20°S, where no AAIW was present in the reference station, and in the presence of the warm salty core of water near 1000 m at 37.4°E (Figure 7). At 20°S, the section did not reach the core of the eddy, which may also account for the lack of a clear signal. However, at 24°S, the waters surrounding the eddy had cooler, fresher, AAIW characteristics, and the differences between the reference station and eddy profiles was distinct. The varying proportions of AAIW in the reference station profiles is likely attributable to the degree of northward penetration by the Mozambique undercurrent.

[30] These differences in reference station profiles were directly reflected in the heat and salt anomalies, which were larger at 24°S (Figures 10 and 11). While the anomalies at 20°S were somewhat ambiguous, at 24°S they clearly represented the difference between RSIW within the eddy and AAIW at the surrounding reference station. Thus we believe these anomaly calculations provide a robust first estimate of the heat and salt content of a Mozambique Channel eddy. The along-isopycnal anomalies represent an accurate estimation of the heat and salt content, because they are not influenced by the vertical displacement of isopycnals caused by eddy Available Potential Energy. Also, since the modification of

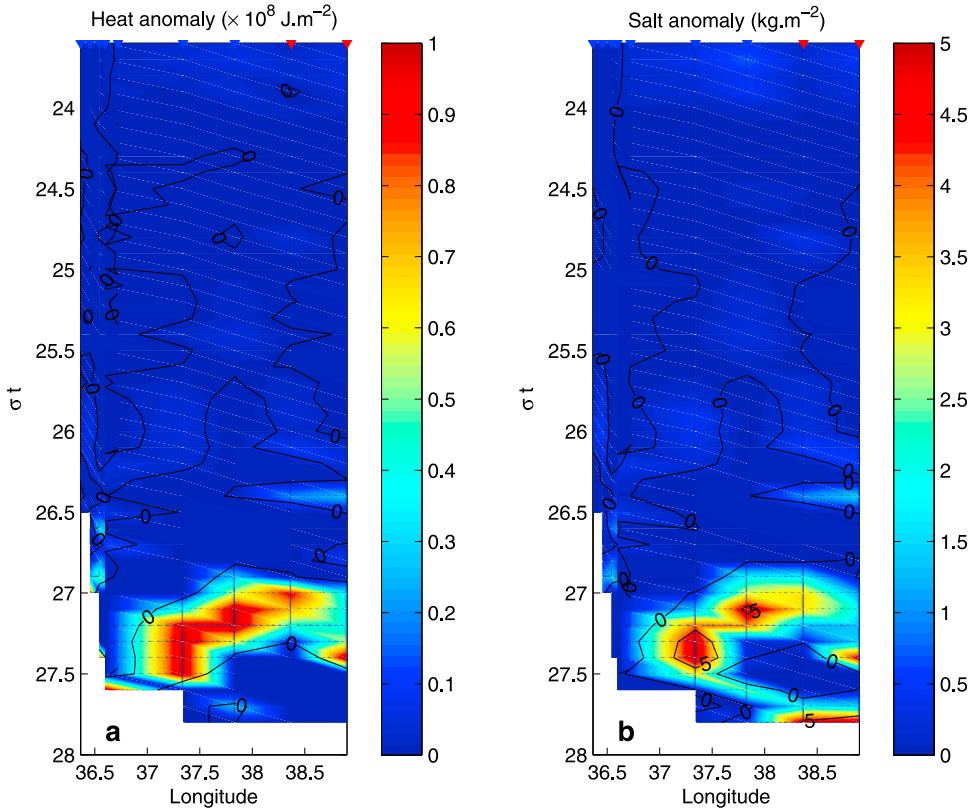

Figure 11. Vertical sections of (a) heat and (b) salt anomalies at 20°S, calculated using isopycnal coordinates. The reference station against which the anomalies were computed was an average of the 7 westernmost stations on the section (blue triangles). The positions of the remaining two stations are shown by the red triangles.

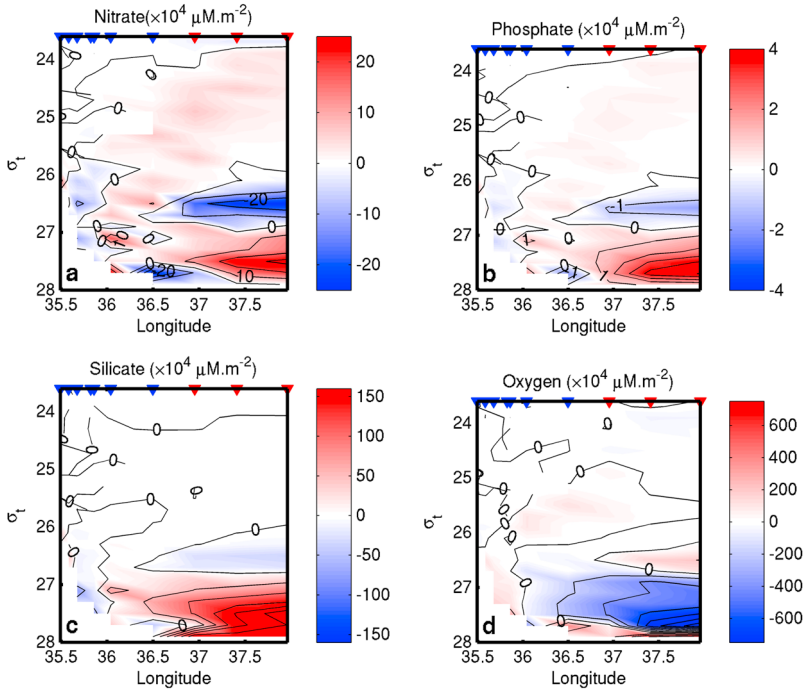

Figure 12. Vertical sections of (a) nitrate, (b) phosphate, (c) silicate, and (d) oxygen anomalies (μM.m^{-2}) at 24°S, in isopycnal coordinates. The anomalies were computed against an average of the 7 westernmost stations on the section (blue triangles). The positions of the remaining stations are shown by the red triangles at top.

Table 1. Total Isopycnal Nutrient Anomalies for the Eddy Found in the Hydrographic Line of Stations Undertaken at 24°S in the Mozambique Channel[a]

Element	Eddy Anomaly (mol)
NO_3^-	1.4×10^{10}
PO_4^-	4.6×10^{9}
SiO_4	3.7×10^{11}
O_2	-9.5×10^{11}

[a]The total anomalies are not consistent with Redfield ratios and should be interpreted with caution (see text for details).

water mass characteristics occurs primarily along isopycnal surfaces, the anomaly calculations are an indication of the eddy's ability to modify the surrounding waters. The magnitude of the anomalies calculated for the eddy at 24°S are comparable to those of Agulhas Rings [*de Ruijter et al.*, 1999a].

[31] The anomaly calculations could have been influenced by the fact that the continental margin was present in the hydrographic sections, and many of the reference profiles lay over the shelf and slope. Indeed most similar anomaly calculations have been carried out for stations occupied in the open ocean, away from the influence of bathymetry [e.g., *Joyce et al.*, 1981; *Swart et al.*, 2008]. Due to the margin bathymetry, the reference stations did not reach as deep as the stations within the eddies, and as noted, were likely influenced by the Mozambique Undercurrent. More data within the channel would be needed to produce a full depth reference station and determine exactly how representative our reference station was. The ASCLME cruises [*Vousden et al.*, 2008] should produce a data set that allows just that.

[32] Regardless of the reference station choice at the two sections, steady southward propagation [*Schouten et al.*, 2003], would carry an eddy increasingly into the domain of AAIW, thus increasing the size of the anomalies. The increase in anomaly size as an eddy advects its ambient RSIW waters further south implies a greater heat and salt flux, as well as an increasing ability to modify the characteristics of surrounding water masses via isopycnal mixing. What is the potential significance of the heat transport by Mozambique Channel eddies to local and global heat budgets?

[33] An eddy heat content of $O(1 \times 10^{20}$ J) with respect to the surrounding water, as calculated, with around 4 eddies per year propagating southward would lead to a divergent eddy heat flux (see *Jayne and Marotzke* [2002] for a definition) of

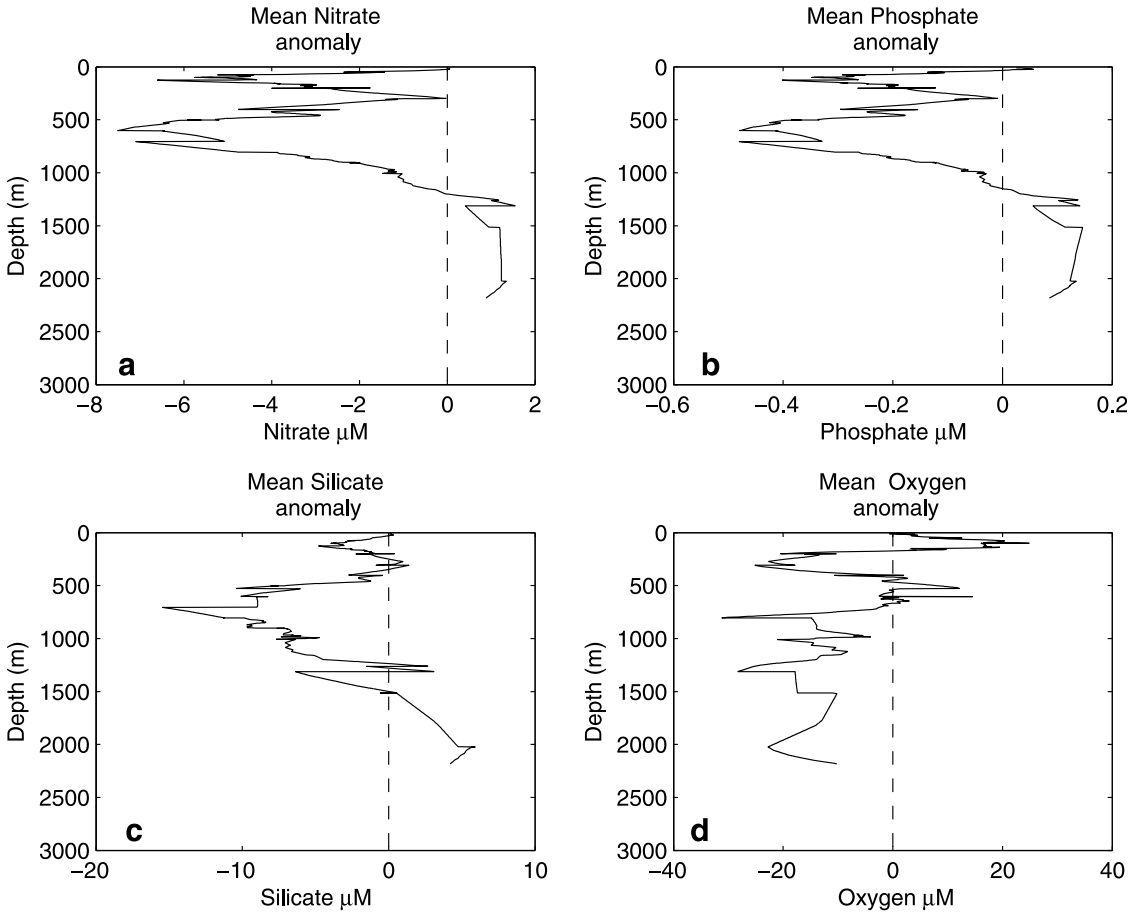

Figure 13. Nutrient anomalies computed in depth coordinates at the hydrographic section undertaken at 24°S in the Mozambique Channel (see also Figures 2, 5, and 6). Note that in the upper 1000 m, the eddies are typically deficient in nutrients at any single depth. This contrasts with the anomaly calculation in isopycnal coordinates (Figure 12) where the eddy represented a positive nutrient anomaly. See the text for a discussion on the relevance of the depth based versus isopycnal based calculation.

$O(4 \times 10^{20}$ J/year = 1.3×10^{13} W) southward over the area of the Mozambique Channel. Through the narrows (400 km wide) this is equivalent to $O(3 \times 10^{7}$ W/m). The flux calculated here represents a fair proportion of the southward divergent eddy heat transport *Jayne and Marotzke* [2002] (Figure 8) have shown for the southern Agulhas Current and for Agulhas Rings entering the South Atlantic ($\leq 1 \times 10^{8}$ W/m).

[34] Previous studies have shown that contributions from the Mozambique Channel significantly influence water mass properties in the Agulhas Current [e.g., *DiMarco et al.*, 2002; *Roman and Lutjeharms*, 2009]. It has also been demonstrated that at least some of these anomalous water signals remain evident as far downstream as Agulhas Rings [*Roman and Lutjeharms*, 2007] and therefore contribute to the flux into the South Atlantic. However, since the majority of Mozambique eddies move poleward outside the Agulhas Current proper [*Schouten et al.*, 2003], and therefore are not absorbed into the Agulhas Current proper, one can currently only speculate on the quantitative contribution they may make to heat and salt flux into the Agulhas Current and hence into the South Atlantic Ocean.

[35] As shown in Figure 13, at any one depth in the upper 1000 m the eddy at 24°S was nutrient poor relative to the surrounding water. This depth-based calculation is the one applicable to biological processes. The negative depth-based nutrient anomalies in the surface waters suggest that the waters within the eddies should have lower rates of primary production than the surrounding waters. However, it has been inferred that the borders of these eddies exhibit high primary productivity since they are preferred foraging areas for marine birds [*Weimerskirch et al.*, 2004]. In contrast, the along isopycnal nutrient anomalies were positive within the eddy, while the oxygen anomaly was negative (Figure 12 and Table 1). As with the heat and salt anomaly, the isopycnal based nutrient calculations reflect the eddy's ability to induce a nutrient flux, and to modify adjacent waters through isopycnal mixing. The large heat, salt and nutrient content of the Mozambique Channel eddies suggests that they are important conveyors of water mass properties.

5. Conclusions

[36] The large, over 200 km diameter, warm eddies observed in the Mozambique Channel during ACSEX I were well matched in size and position with altimetrically derived, positive sea level anomalies. The altimetry, LADCP measurements, geostrophic calculations and surface velocity profilers concurred on the strong anti-cyclonic rotation of the features. The strong geostrophic currents were related to a bowl-like displacement of the isopynals, which descended vertically by 100 m from the edges of these feature to their centers. The southernmost eddy contained significant amounts of heat and salt, on a par with Agulhas Rings. Along isopycnal surfaces, it was also enriched in nutrients relative to the surrounding waters. In contrast, the eddy was depleted oxygen. These strong anomalies suggest that the Mozambique Channel eddies may influence the water mass characteristics of the Agulhas Current [e.g., *Roman and Lutjeharms*, 2009] into which they may partially and intermittently feed, and perhaps ultimately the physical and chemical properties of the South Atlantic basin via Agulhas leakage [e.g., *Roman and Lutjeharms*, 2007].

[37] **Acknowledgments.** We thank the South African National Research Foundation as well as the University of Cape Town for funding and express our gratitude to the captain and the crew of the RV *Pelagia* for solid and enthusiastic support during the ACSEX cruises. JREL thanks the Leibnitz-Insitut für Meereswissenschaften in Kiel for hospitality during a sabbatical when this work was completed.

References

Biastoch, A., and W. Krauss (1999), The role of mesoscale eddies in the source regions of the Agulhas Current, *J. Phys. Oceanogr.*, *29*, 2303–2317, doi:10.1175/1520-0485(1999)029<2303:TROMEI>2.0.CO;2.

Biastoch, A., J. R. E. Lutjeharms, C. W. Bőning, and M. Scheinert (2008a), Mesoscale perturbation control inter-ocean exchange south of Africa, *Geophys. Res. Lett.*, *35*, L20602, doi:10.1029/2008GL035132.

Biastoch, A., C. W. Böning, and J. R. E. Lutjeharms (2008b), Agulhas leakage dynamics affects decadal variability in Atlantic overturning circulation, *Nature*, *456*, 489–492, doi:10.1038/nature07426.

Biastoch, A., L. Beal, J. R. E. Lutjeharms, and T. G. D. Casal (2009), Variability and coherence of the Agulhas Undercurrent in a high-resolution Ocean General Circulation Model, *J. Phys. Oceanogr.*, *39*, 2417–2426, doi:10.1175/2009JPO4184.1.

Clowes, A. J., and G. E. R. Deacon (1935), The deep-water circulation of the Indian Ocean, *Nature*, *136*, 936–938, doi:10.1038/136936a0.

de Ruijter, W. P. M., A. Biastoch, S. S. Drijfhout, J. R. E. Lutjeharms, R. P. Matano, T. Pichevin, P. J. van Leeuwen, and W. Weijer (1999a), Indian-Atlantic interocean exchange: Dynamics, estimation and impact, *J. Geophys. Res.*, *104*, 20,885–20,910, doi:10.1029/1998JC900099.

de Ruijter, W. P. M., P. J. van Leeuwen, and J. R. E. Lutjeharms (1999b), Generation and evolution of Natal Pulses: Solitary meanders in the Agul has Current, *J. Phys. Oceanogr.*, *29*, 3043–3055, doi:10.1175/1520-0485(1999)029<3043:GAEONP>2.0.CO;2.

de Ruijter, W. P. M., H. Ridderinkhof, J. R. E. Lutjeharms, M. Schouten, and C. Veth (2002), Observations of flow in the Mozambique Channel, *Geophys. Res. Lett.*, *29*(10), 1502, doi:10.1029/2001GL013714.

de Ruijter, W. P. M., G. J. A. Brummer, S. S. Drijfhout, J. R. E. Lutjeharms, F. Peeters, H. Ridderinkhof, H. M. van Aken, and P. J. van Leeuwen (2006), Observations of the inter-ocean exchange around South Africa, *Eos Trans. AGU*, *87*, 97–101, doi:10.1029/2006EO090002.

DiMarco, S. F., P. Chapman, W. D. Nowlin, P. Hacker, K. Donohue, M. Luther, G. C. Johnson, and J. Toole (2002), Volume transport and property distributions of the Mozambique Channel, *Deep Sea Res. Part II*, *49*, 1481–1511, doi:10.1016/S0967-0645(01)00159-X.

Donohue, K., and J. Toole (2003), A near-synoptic survey of the Southwest Indian Ocean, *Deep Sea Res. Part II*, *50*, 1893–1931, doi:10.1016/S0967-0645(03)00039-0.

Gordon, A. L. (1985), Indian-Atlantic transfer of thermocline water at the Agulhas retroflection, *Science*, *227*, 1030–1033, doi:10.1126/science.227.4690.1030.

Grasshoff, K., M. Ehrhardt, and K. Kremling (1983), *Methods of Seawater Analysis*, 2nd ed., Chemie, Weinheim, Germany.

Harlander, U., H. Ridderinkhof, M. W. Schouten, and W. P. M. de Ruijter (2009), Long-term observations of transport, eddies, and Rossby waves in the Mozambique Channel, *J. Geophys. Res.*, *114*, C02003, doi:10.1029/2008JC004846.

Jayne, S. R., and J. Marotzke (2002), The oceanic eddy heat transport, *J. Phys. Oceanogr.*, *32*, 3328–3345, doi:10.1175/1520-0485(2002)032<3328:TOEHT>2.0.CO;2.

Joyce, T., S. Patterson, and R. Millard (1981), Anatomy of a cyclonic ring in the Drake Passage, *Deep Sea Res. Part I*, *28A*, 1265–1287.

Lutjeharms, J. R. E. (2006), *The Agulhas Current*, 329 pp., Springer, Berlin.

Lutjeharms, J. R. E., P. M. Wedepohl, and J. M. Meeuwis (2000), On the surface drift of the East Madagascar and the Mozambique Currents, *S. Afr. J. Sci.*, *96*, 141–147.

Michaelis, G. (1923), Die wasserbewegung an der oberfläche des Indischen Ozeans im Januar und Juli, *Rep. A8(16)*, 32 pp., Inst. fur Meereskd., Univ. Berlin, Berlin.

Morrow, R., J. R. Donguy, A. Chaigneau, and S. R. Rintoul (2004), Cold-core anomalies at the subantarctic front, south of Tasmania, *Deep Sea Res. Part I*, *51*, 1417–1440.

Palastanga, V., P. J. van Leeuwen, M. W. Schouten, and W. P. M. de Ruijter (2007), Flow structure and variability in the subtropical Indian Ocean:

Instability of the South Indian Ocean Countercurrent, *J. Geophys. Res.*, *112*, C01001, doi:10.1029/2005JC003395.

Peterson, R. G., W. D. Nowlin, and T. Whitworth (1982), Generation and evolution of a cyclonic ring at Drake Passage in early 1979, *J. Phys. Oceanogr.*, *12*, 712–719, doi:10.1175/1520-0485(1982)012<0712:GAEOAC>2.0.CO;2.

Quartly, G., and M. Srokosz (2004), Eddies in the southern Mozambique Channel, *Deep Sea Res. Part II*, *51*, 69–83, doi:10.1016/j.dsr2.2003.03.001.

Ridderinkhof, H. (2000), RV *Pelagia* cruise report, cruise 64PE156, project ACSEX-I, report, R. Neth. Inst. for Sea Res., Texel, Netherlands.

Ridderinkhof, H., and W. de Ruijter (2003), Moored current observations in the Mozambique Channel, *Deep Sea Res. Part II*, *50*, 1933–1955, doi:10.1016/S0967-0645(03)00041-9.

Ridderinkhof, H., J. R. E. Lutjeharms, and W. P. M. de Ruijter (2001), A research cruise to investigate the Mozambique Current, *S. Afr. J. Sci.*, *97*, 461–464.

Roman, R. E., and J. R. E. Lutjeharms (2007), Red Sea Intermediate Water at the Agulhas Current termination, *Deep-Sea Res. Part I*, *54*, 1329–1340.

Roman, R. E., and J. R. E. Lutjeharms (2009), Red Sea Intermediate Water in the source regions of the Agulhas Current, *Deep Sea Res. Part I*, *56*, 939–962.

Sætre, R., and A. Jorge da Silva (1984), The circulation of the Mozambique Channel, *Deep Sea Res.*, *31*, 508–585.

Schouten, M., W. de Ruijter, and P. van Leeuwen (2002a), Upstream control of Agulhas Ring shedding, *J. Geophys. Res.*, *107*(C8), 3109, doi:10.1029/2001JC000804.

Schouten, M., W. de Ruijter, P. van Leeuwen, and H. Dijkstra (2002b), An oceanic teleconnection between the equatorial and southern Indian Ocean, *Geophys. Res. Lett.*, *29*(16), 1812, doi:10.1029/2001GL014542.

Schouten, M., W. de Ruijter, P. van Leeuwen, and R. Ridderinkhof (2003), Eddies and variability in the Mozambique Channel, *Deep Sea Res. Part II*, *50*, 1987–2003, doi:10.1016/S0967-0645(03)00042-0.

Siedler, G., M. Rouault, and J. R. E. Lutjeharms (2006), Structure and origin of the subtropical South Indian Ocean Countercurrent, *Geophys. Res. Lett.*, *33*, L24609, doi:10.1029/2006GL027399.

Siedler, G., M. Rouault, A. Biastoch, B. Backeberg, C. J. C. Reason, and J. R. E. Lutjeharms (2009), Modes of the southern extension of the East Madagascar Current, *J. Geophys. Res.*, *114*, C01005, doi:10.1029/2008JC004921.

Swart, N. C., I. J. Ansorge, and J. R. E. Lutjeharms (2008), Detailed characterization of a cold Antarctic eddy, *J. Geophys. Res.*, *113*, C01009, doi:10.1029/2007JC004190.

van Aken, H. M., H. Ridderinkhof, and W. P. M. de Ruijter (2004), North Atlantic Deep Water in the south-western Indian Ocean, *Deep Sea Res. Part I*, *51*, 755–776, doi:10.1016/j.dsr.2004.01.008.

van Ballegooyen, R. C., M. L. Gründlingh, and J. R. E. Lutjeharms (1994), Eddy fluxes of heat and salt from the southwest Indian Ocean into the southeast Atlantic Ocean: A case study, *J. Geophys. Res.*, *99*, 14,053–14,070, doi:10.1029/94JC00383.

van Leeuwen, P. J., W. P. M. de Ruijter, and J. R. E. Lutjeharms (2000), Natal pulses and the formation of Agulhas rings, *J. Geophys. Res.*, *105*, 6425–6436, doi:10.1029/1999JC900196.

Vousden, D., L. E. P. Scott, W. Sauer, T. Bornman, M. Ngoile, J. Stapley, and J. R. E. Lutjeharms (2008), Establishing a basis for ecosystem management in the western Indian Ocean, *S. Afr. J. Sci.*, *104*, 417–420.

Weijer, W., W. P. M. de Ruijter, H. A. Dijkstra, and P. J. van Leeuwen (1999), Impact of interbasin exchange on the Atlantic Overturning Circulation, *J. Phys. Oceanogr.*, *29*, 2266–2284, doi:10.1175/1520-0485(1999)029<2266:IOIEOT>2.0.CO;2.

Weimerskirch, H., M. le Corre, S. Jaquemet, M. Potier, and F. Marsac (2004), Foraging strategy of a top predator in tropical waters: Great frigatebirds in the Mozambique Channel, *Mar. Ecol. Prog. Ser.*, *275*, 297–308, doi:10.3354/meps275297.

W. P. M. de Ruijter, Institute for Marine and Atmospheric Research, Utrecht University, Princetonplein 5, NL-3584 CC Utrecht, Netherlands.

J. R. E. Lutjeharms, Department of Oceanography, University of Cape Town, Private Bag X3, Rondebosch, Cape Town 7701, South Africa.

H. Ridderinkhof, Royal Netherlands Institute for Sea Research, PO Box 59, NL-1790 AB, Texel, Netherlands.

N. C. Swart, School of Earth and Ocean Sciences, University of Victoria, PO Box 3065 STN CSC, Victoria, BC V8W 3V6, Canada. (ncswart@uvic.ca)